A LOV Story: The Signaling State of the Phot1 LOV2 Photocycle Involves Chromophore-Triggered Protein Structure Relaxation, As Probed by Far-UV Time-Resolved Optical Rotatory Dispersion Spectroscopy†

Eefei Chen,* Trevor E. Swartz, Roberto A. Bogomolni, and David S. Kliger

Department of Chemistry and Biochemistry, University of California, Santa Cruz, California 95064

Received December 11, 2006; Revised Manuscript Received February 2, 2007

ABSTRACT: Light-, oxygen-, or voltage-regulated (LOV1 and LOV2) domains bind flavin mononucleotide (FMN) and activate the phototropism photoreceptors phototropin 1 (phot1) and phototropin 2 (phot2) by using energy from absorbed blue light. Upon absorption of blue light, chromophore and protein conformational changes trigger the kinase domain for subsequent autophosphorylation and presumed downstream signal transduction. To date, the light-induced photocycle of the phot1 LOV2 protein is known to involve formation of a triplet flavin mononucleotide (FMN) chromophore followed by the appearance of a FMN adduct within 4 μs [Swartz, T. E., Corchnoy, S. B., Christie, J. M., Lewis, J. W., Szundi, I., Briggs, W. R., and Bogomolni, R. A. (2001) *J. Biol. Chem. 276*, 36493−36500] before thermal decay back to the dark state. To probe the mechanism by which the blue light information is relayed from the chromophore to the protein, nanosecond time-resolved optical rotatory dispersion (TRORD) spectroscopy, which is a direct probe of global secondary structure, was used to study the phot1 LOV2 protein in the far-UV region. These TRORD experiments reveal a previously unobserved intermediate species ($\tau \sim 90$ μs) that is characterized by a FMN adduct chromophore and partially unfolded secondary structure (LOV_{390}^{S2}). This intermediate appears shortly after the formation of the FMN adduct. For LOV2, formation of a long-lived species that is ready to interact with a receptor domain for downstream signaling is much faster by comparison with formation of a similar species in other light-sensing proteins.

Environmental light conditions regulate many of the growth and developmental responses in plants. These phenomena are controlled by different photoreceptors that are sensitive to different wavelengths and intensities of light. For example, phytochrome A absorbs primarily red and far-red light, whereas cryptochrome and phototropin are selective for blue light. Together with phytochrome, cryptochrome regulates photomorphogenetic processes such as seed germination, flowering, stem elongation, and gene expression. Phototropism, stomatal opening, relocation of chloroplasts, and other photomovements are controlled by the phototropins (*1*−*6*).

Phototropin 1 (phot1)[1] is a 996-amino acid membrane-associated kinase flavoprotein that undergoes autophosphorylation upon irradiation with blue light (*6*). The domain configuration of phot1 comprises a serine-threonine kinase segment at the C-terminal end and two 12 kDa (110 amino acids) light-, oxygen-, or voltage-regulated (LOV1 and LOV2) segments in the N-terminal region. Being a member of the PAS (Per-ARNT-Sim) domain superfamily, LOV domains have a distinctive structure. A five-stranded antiparallel β-sheet core ($\beta_2\alpha_4\beta_3$), flanked by a series of helical segments, facilitates its characteristic functions of light detection, chromophore binding, and signal transduction via protein−protein interactions. For phot1, both LOV1 and LOV2 domains bind a flavin mononucleotide (FMN) chromophore and LOV2 activates phototropin by converting detected blue light into a protein conformational change (*7*−*10*). Upon absorbing blue light, the FMN chromophore of the isolated LOV2 domain has been shown to form a triplet state ($\lambda_{max} \sim 660$ nm) via intersystem crossing directly from the excited singlet state within 5 ns (*11*). These femtosecond time-resolved absorption studies also used different pH conditions to demonstrate that a large population of the FMN triplets exists in the protonated state. Excited state proton transfer from the sulfhydryl group of the Cys39 to the N(5) of the FMN chromophore is thus proposed to occur on a nanosecond or faster time scale (*11*) and to facilitate formation of a C39−C(4a) flavin−cysteinyl adduct (*12*). The results of nanosecond time-resolved absorption experiments show that the FMN triplet state decays with a 4 μs time constant[2] to form the FMN adduct ($\lambda_{max} \sim 390$ nm) (*7*). The FMN adduct was proposed to be the active signaling state, in part because it is sufficiently long-lived

† Supported by National Institutes of Health Grant EB02056 (D.S.K.) and NSF Grant MCB 0444390 (R.A.B.).

* To whom correspondence should be addressed. Phone: (831) 459-4007. Fax: (831) 459-2935. E-mail: chen@chemistry.ucsc.edu.

[1] Abbreviations: phot1, phototropin 1; LOV, light-, oxygen-, and voltage-regulated; PAS, Per-ARNT-Sim; FMN, flavin mononucleotide; PYP, photoactive yellow protein; TRORD, time-resolved optical rotatory dispersion; TROD, time-resolved absorption; SVD, singular-value decomposition.

[2] The time constant measured by Swartz et al. (*9*) was 2 μs. When the decay of the triplet state back to the ground state is considered, the calculated time constant for adduct formation is 4 μs. This value will be used throughout the paper.

10.1021/bi602544n CCC: $37.00
Published on Web 03/20/2007

to transmit the information of blue light absorption to the kinase domain and in part because no additional intermediate has been detected between its formation and its decay back to the dark state [$\tau_{1/2} \sim 30$ s (*12*)].

Many questions regarding the mechanistic and conformational details of the phot1 LOV2 photocycle remain. For example, do the chromophore and protein respond simultaneously upon absorption of blue light, or do the initial FMN-localized structural changes propagate through the core sheet structure and then communicate a conformational change in the outlying helical structure? Do hydrophobic contacts play a larger role in facilitating such structural change sequences than steric hindrance or distortion of the chromophore? The answers to such questions will not only provide mechanistic information about the LOV2 photocycle but also help in identifying commonalities in the mechanisms of signal transduction activation for PAS, as well as non-PAS, proteins.

At present, common elements in signaling mechanisms of different proteins include an initial conformational change that is localized to the chromophore site, distortion of the protein structure in the proximity of the chromophore, and then propagation of this distortion to a long-range protein structure such as the N- and C-terminal helices. For example, in the prototypical PAS domain protein, photoactive yellow protein (PYP), the sequence of structural changes that occurs upon absorption of light is at first localized to the chromophore pocket. Complete relaxation of the *cis* chromophore geometry results in the cleavage of all hydrogen bonds that link the chromophore to helix B. Helix B subsequently moves toward the N-terminal helix, which responds by unfolding to form the signaling state (*13*). Studies of phytochrome A activation have proposed that the chromophore rearrangement following the initial photoisomerization step may introduce strain on the protein that is manifested in part as a helical change (unfolding) at the N-terminus. When N-terminal residues 7−69 are cleaved, the resulting mutant phytochrome A exhibits no biological activity (*14*), suggesting that the partially unfolded N-terminus interacts with the primary signaling partners, phytochrome-interacting factors (*15*).

The protein−protein interaction of a signaling partner protein with a helical domain appears to be significant in the mechanism of signal transduction. In addition to the helical unfolding observed during the formation of the signaling state in PYP and phytochrome, helical segments also appear to play a significant role in the signaling pathway for other proteins such as the oxygen-sensor protein FixL (*16*, *17*), the quorum-sensing protein TraR (*18*, *19*) and the HERG voltage-dependent potassium channel (*20*). In the LOV2 protein, it was recently shown that the Jα helix, which is located at the end immediately C-terminal to the $\beta_2\alpha_4\beta_3$ PAS domain core and is aligned with the β-sheet surface of the core, is critical for light-activated kinase activity (*9*, *10*). From these NMR studies, it was proposed that irradiation leads to adduct formation, disruption of the interaction between the core β-sheet and the Jα helix, and then unfolding of helix Jα. Consistent with these findings, steady-state light-induced difference CD spectra show a loss of α-helicity (*8*).

The goal of this study is to probe the kinetics of the LOV2 protein changes during its photocycle by using far-UV nanosecond time-resolved optical rotatory dispersion (TRORD) spectroscopy, which follows global protein secondary structure. The results of these experiments indicate that upon photoexcitation with 355 nm light the observed secondary structure unfolding ($\tau = 90$ μs), presumably localized to the Jα helix, is facilitated by the previously observed FMN adduct formation event [$\tau = 4$ μs (*7*)].

MATERIALS AND METHODS

Sample Preparation. The LOV2 domain [AsNPH1LOV2 (amino acids 404−559)] used in these experiments was derived from oat (*Avena sativa*) phot1. This LOV2 construct includes the Jα helix region that undergoes unfolding upon irradiation with light (*9*). It was expressed in *Escherichia coli* and purified by calmodulin affinity chromatography (using an N-terminal tag) (Stratagene, La Jolla, CA). The purified samples were washed into clean buffer [5 mM TRIS and 5 mM NaCl (pH 8)] using centrifugal concentrators (Continental Lab Products, San Diego, CA) and were centrifuged and/or filtered through a 0.2 μm filter prior to use. Absorption spectra of the LOV2 protein were measured on an HP8452 diode array spectrophotometer (Hewlett-Packard, Palo Alto, CA). The concentration of the protein was calculated using an $\epsilon_{447,LOV2}$ of 13 800 M^{-1} cm^{-1}. Further details of the sample preparation have been reported (*8*, *12*, *21*).

For time-resolved experiments, the LOV2 samples were diluted with enough buffer solution [5 mM TRIS and 5 mM NaCl (pH 8)] so that the absorption value at 230 nm was 0.5−0.6 (∼15 μM protein) in a 2 mm path length quartz cuvette. This concentration of protein is below that at which dimerization of phot1 LOV2 reportedly plays a role in the dark state (50−200 μM) and during the photocycle (*22*, *23*).

Time-Resolved Optical Rotatory Dispersion and Absorption Experiments. The TRORD apparatus has been described in detail elsewhere (*24*) and will be discussed briefly here. The TRORD system comprises two major components, the photoexcitation source for initiation of the reaction and the probe source for following the subsequent time-dependent spectral changes. Pulses of 355 nm light (∼7 ns, full width at half-maximum) from a Q-switched Quanta Ray DCR-1 Nd:YAG laser were used to initiate the cyclic phot1 LOV2 photoreactions. The phot1 LOV2 photocycle has typically been initiated with ca. 470 nm light in previous time-resolved studies (*7*, *8*, *11*, *23*). Because 355 nm light was used to trigger the photocycle in these far-UV TRORD studies, the power dependence of the absorption changes at 270 nm was examined to establish that 1−1.5 mJ was the optimum energy per pulse for the experiments (data not shown). An iris was used to reduce the unfocused 6−7 mm laser beam diameter to ∼3 mm. The ∼3 mm laser beam entered the sample at an angle of 15° where it overlapped with the ∼300 μm probe beam. The initially unpolarized probe light from a xenon flash lamp probe source passed through a MgF_2 polarizer to a UV-enhanced aluminum spherical mirror (F/2, Edmund Optics), which focused the probe light at the sample. After the sample, the probe light passed to a second UV-enhanced aluminum spherical mirror and a second MgF_2 polarizer. The probe beam was then focused onto the slit of a spectrograph (Monospec 27, Thermo Jarrell Ash, Franklin, MA) equipped with a 600 groove/mm grating (200 nm blaze) and detected with a CCD (iStar, Andor Technology, South Windsor, CT). ORD signals were obtained by measuring the intensities of

the probe beam after the first polarizer had been rotated by angles of $+\beta$ and then $-\beta$ off the crossed position (90°) of the two polarizers.

Aliquots of LOV2 protein (3 mL) were used for each experiment. The LOV2 sample was transported with a peristaltic pump to a 2 mm quartz flow cell and then out to a collection vial. Because the half-life of the LOV2 back reaction is ~30 s, the sample remained in the collection vial until the entire aliquot had been used. This waiting period allowed the sample to return to the dark state so that it could be recycled for further data collection.

Far-UV TRORD data were collected in two groups using two different LOV2 preparations. For the "late" data group, measurements were obtained at the following time delays: 2, 11, 100, and 500 μs, 1, 5, 10, 50, 100, and 200 ms, and 1 s. A total of 336−464 averages were accumulated at each time delay. In the second "early" data group, the time delays were clustered in the submillisecond time region: 3, 4, 6, 10, 18, 34, 66, and 100 μs, where at each time delay 728−760 averages were collected. For each time delay that was measured, an initial, dark-state ORD signal was also obtained. For both groups, all time points were collected within each run of the entire aliquot. The data were collected at a repetition rate of 0.5 Hz, with the sample flowing (only between laser pulses) at a rate of 8−9 μL/s to move the irradiated sample out of the pump−probe path before the next laser pulse. That this flow rate is sufficient for minimizing the buildup of photoproduct is verified by measuring TROD spectra with similar band intensities at an arbitrary time delay.

TROD and TRORD data were accumulated simultaneously in the 210−310 nm wavelength region. Thus, the far-UV TRORD and near-UV TROD data for the 230 nm band were measured at the same time points within each data group (early and late). However, only the early near-UV TROD data are shown below. In total, approximately 1000 averages were accumulated at each time delay for the 270 nm band TROD data.

Prior to the experiments, an UV−vis spectrum of the dark state of LOV2 was measured on a Shimadzu (Columbia, MD) UV-2101PC spectrophotometer using a 2 mm path length quartz cuvette. At the end of each experiment, a second UV−vis spectrum was measured to determine the integrity of the protein. Temperature measurements were made periodically throughout the experiment with an infrared temperature probe (80T-IR, Fluka). The temperature at the sample was maintained at 24 °C during the course of the experiment. All experiments were performed in a dark environment.

Data Analysis. Singular-value decomposition (SVD) and global analysis methods were used to analyze the multiwavelength difference TROD and TRORD data. The difference data were obtained by subtracting the initial, dark-state LOV2 spectrum from the time-resolved OD and OR spectra. For the TRORD data, difference kinetic traces were also obtained by averaging the multiwavelength difference ORD signals from 225 to 235 nm. The resulting difference kinetic traces were analyzed using exponential fitting methods. Algorithms for all methods (exponential, SVD, and global analysis) were written with the mathematical software package Matlab (The Mathworks, Inc., South Natick, MA). Further details of SVD and global analyses of kinetic spectral data are reported elsewhere (*25*). The reported error bars for each time point are the calculated standard deviations of the ORD signal mean value, which was based on the average of 42−58 and 91−95 sets (of eight averages each) of data depending on the time point measured, for the late and early data groups, respectively.

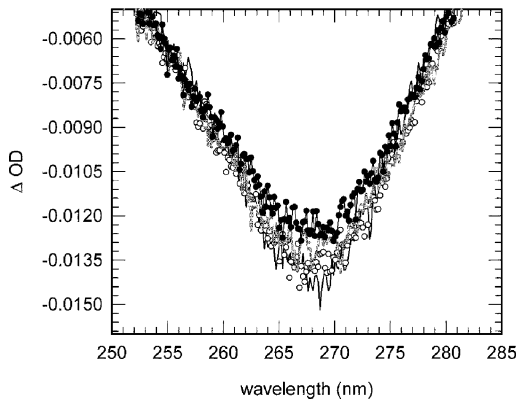

FIGURE 1: Near-UV TROD data for the phot1 LOV2 photocycle. The 270 nm band reflects absorption not only by the FMN chromophore but also by aromatic amino acids such as Tyr and Trp. Thus, the dynamics of this band will provide information about whether time-dependent changes in the corresponding TRORD signals are due to the chromophore alone or to both the chromophore and the protein. The figure shows only TROD data measured at 3 (black line), 6 (white circles), 34 (gray line), and 100 μs (thin black line with black circles). Analysis of all the data yields a single-exponential decay component with a lifetime of 3 ± 1 μs. Because 50% of the triplet state returns to the ground state and the other 50% decays to the adduct, τ_1 is equal to τ_2 and is twice τ_{obs}. Consequently, $\tau_1 = \tau_2 = 6 \pm 2$ μs.

During ORD experiments, intensity measurements are accumulated at each position of β with [$I_{\lambda(+\beta)}$ and $I_{\lambda(-\beta)}$] and without [$I^0_{\lambda(+\beta)}$ and $I^0_{\lambda(-\beta)}$] the laser light and stored. At each position of the polarizer, a TROD spectrum is calculated from the log of the ratio of the intensity measurements obtained without and with the laser at each time delay. ORD are calculated from the signal (S_λ = ORD/2β) according to the relations $S_\lambda = [I_{\lambda(+\beta)} - I_{\lambda(-\beta)}]/[I_{\lambda(+\beta)} + I_{\lambda(-\beta)}]$ for the time-resolved data and $S^0_\lambda = [I^0_{\lambda(+\beta)} - I^0_{\lambda(-\beta)}]/[I^0_{\lambda(+\beta)} + I^0_{\lambda(-\beta)}]$ for the pretrigger data.

RESULTS

The near-UV 270 nm band largely reflects the absorption characteristics of the FMN chromophore. Some of the TROD data measured at 3, 4, 6, 10, 18, 34, 66, and 100 μs are shown in Figure 1. Global kinetic analyses show that near-UV TROD data for the 270 nm band are best fit to a single-exponential decay with an observed time constant of 3 ± 1 μs. This time constant (τ_{obs}) reflects the sum of the time constants for the decay of the triplet state to the ground state (τ_1) and the formation of the FMN adduct (τ_2) (*7*). Because 50% of the triplet state returns to the ground state and the other 50% decays to the adduct, τ_1 is equal to τ_2 and is twice τ_{obs}. Consequently, $\tau_1 = \tau_2 = 6 \pm 2$ μs. This value is consistent with the 4 μs decay time constant reported by Swartz et al. (*7*), and as with the 4 μs process, the 6 μs component is attributed to the dynamics of the FMN chromophore as it decays from the triplet state. These data confirm that the early photocycle kinetics of LOV2 initiated by 355 nm light (in this study) can be compared with the

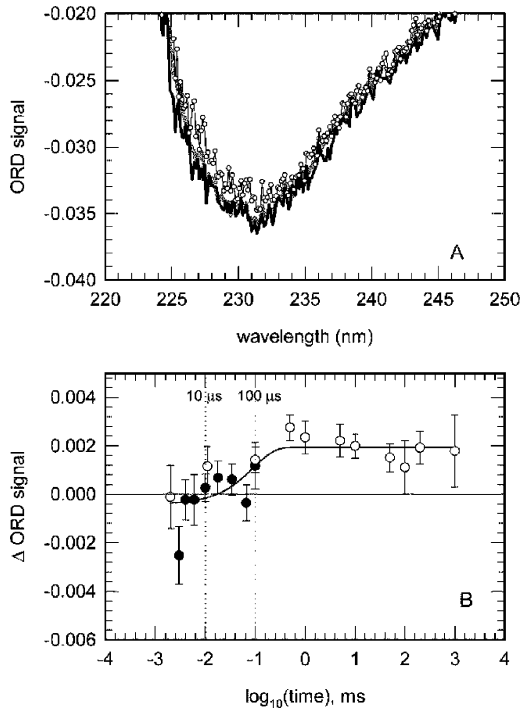

FIGURE 2: Far-UV TRORD data for the phot1 LOV2 photocycle. Multichannel-detected ORD signals measured before illumination (gray line) and at 4 (black line) and 100 μs (thin black line with white circles) after illumination are shown in panel A. Data at only a few time points are shown because the change in signal is small (6−8%). TRORD kinetic trace data measured using the time delays from both the late (○) and early (●) data groups are shown in panel B, with the fit to the data. Analysis of the combined early and late data groups gives a single-exponential process with a time constant of 90 ± 36 μs.

kinetics reported after 477 nm excitation. They are consistent with the observation by Guo et al. (*26*) of similar changes in the 475 nm absorption bleaching with visible (tungsten lamp) and UV (280−390 nm) light. TROD data were also measured in the visible (450 nm) region but are not shown here. The fit of those data was consistent with the previously published work of Swartz et al. (*7*).

Figure 2A shows the multichannel-detected ORD signals measured before and 4 and 100 μs after photoexcitation with 355 nm light. Two time delays are shown because the maximum change in signal is only 6−8%. The TRORD data at all time points are shown in the form of a difference kinetic trace in Figure 2B. The late data measurements at 2, 11, 100, and 500 μs, 1, 5, 10, 50, 100, and 200 ms, and 1 s (○) are presented along with the early data measured at 3, 4, 6, 10, 18, 34, 66, and 100 μs (●). From the late data, the decrease in the magnitude of the ORD signal triggered by blue light absorption appears to be ∼70% complete within 10−100 μs, with the remaining 30% decrease in magnitude occurring before ∼1 ms. The early time measurements resolve the data at times faster than 100 μs and show a general trend in which the magnitude of the ORD signal decreases from 4 to 100 μs. The 11 μs (○) time point from the late data set shows a more intense ΔORD signal but is within the error of the 10 μs point (●) from the early data set. At 100 μs, the ΔORD signals are very similar in intensity. The combined late and early data set is best fit to a single-exponential decay with a time constant of 90 ± 36 μs.[3] The error bar on the time constant was calculated on the basis of the values obtained from analysis of different sets of the late and early data.

It was also possible to fit two-exponential processes to the data (ca. 4 and 180 μs); however, the time-dependent spectral components, generated by SVD and global kinetic analysis (*25*), of the two intermediates were nearly identical. The similarity of the 4 μs time constant to that detected in the near-UV TROD data and the data reported by Swartz et al. (*7*) suggests that the ORD signal at 230 nm may also reflect the dynamics of formation of the chromophore adduct. This is possible because in kinetic ORD measurements the signals are monitored away from the absorption bands. Consequently, the ORD signal at 230 nm comprises multiple Cotton effects, and in this case, it may report on the contribution of the chromophore absorption band at 270 nm. Given the size of the error bars for each time delay, detection of two exponential processes within a 6−8% change can only be certain with a better signal-to-noise ratio. Thus, at this time, a single-exponential decay ($\tau = 90 \pm 36$ μs) is reported and is attributed to changes in protein secondary structure.

DISCUSSION

In phot1 LOV2, the amphipathic Jα helix structure, found at the C-terminal side of the LOV2 $\beta_2\alpha_4\beta_3$ core, is believed to play a significant role in signaling activation (*9*). Partial unfolding of the Jα helix is consistent with the observed decrease in the far-UV CD spectra upon white light illumination of LOV2 (*8*). The kinetics of the LOV2 photocycle, with a focus on the secondary structure changes, were studied here with TRORD methods in an effort to understand the relative time scales of chromophore and protein structural changes upon irradiation with blue light. The near-UV TROD data report a lifetime of 6 ± 2 μs, which is attributed to changes in the chromophore and is consistent with previous studies [$\tau = 4$ μs (*7*)]. This intermediate is termed $LOV2_{390}{}^{S1}$, which is modified slightly from the nomenclature initially introduced (*7*) to accommodate the new intermediate observed in this study. The far-UV TRORD data suggest that the decrease in secondary structure content occurs (presumably at the Jα helix) after formation of the FMN adduct, with a time constant of ∼90 μs. The species observed at 90 μs is characterized by a FMN adduct with partly unfolded helical structure and is called $LOV2_{390}{}^{S2}$. Because the far-UV TRORD and near-UV TROD measurements were accumulated for the same sample, at the same time, and with the same time delays, there are no ambiguities about the assignments of the time constants. Overall, the results of the TRORD and TROD studies on phot1 LOV2 (including the linker region) indicate that soon after formation of the FMN adduct there is a decrease in secondary structure content.

The 90 μs time constant for the secondary structure change is much faster than the time constant of 2 ms reported in laser-induced transient grating (TG) studies (*27*). A possible explanation for the different time constants is that TG is not as sensitive to changes in the protein structure as TRORD. TG techniques indirectly probe protein conformational changes by monitoring the translational diffusion coefficient

[3] When Figure 2B is plotted with a linear scale, the fit of the data exhibits the exponential rise that is expected.

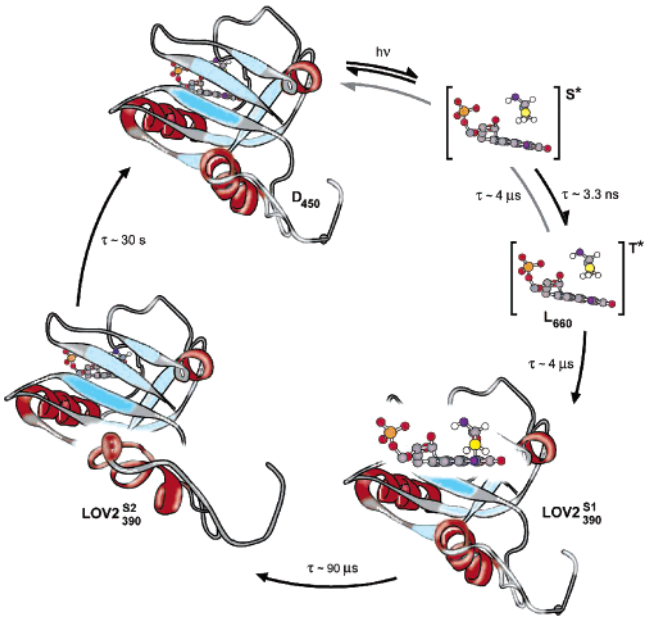

FIGURE 3: Phot1 LOV2 photocycle. The phot1 LOV2 photocycle intermediates observed to date are summarized here. The newest intermediate, named $LOV2_{390}^{S2}$, can be described as having a FMN adduct chromophore and partly unfolded protein structure. The excited singlet and triplet (L_{660}) states of the FMN are shown without the protein structure to emphasize that the dynamics are localized to the chromophore. The drawings of the intermediate species, $LOV2_{390}^{S1}$ and $LOV2_{390}^{S2}$, zoom in on where the major changes occur (which are highlighted), at the chromophore and at the protein, respectively.

parameter (*D*) (*27*, *28*), whereas TRORD methods report on the global secondary structure changes of the protein. According to the analysis of the observed TG signal by Eitoku et al., using a two-state model resulted in a poor fit of the data. This problem was addressed by invoking an unusual time dependence of *D* in the analysis. However, examination of their biexponential fit (Figure 3 in ref *27*) shows that deviation from the observed TG signal starts in approximately the same time region as the 90 μs time constant reported from the far-UV TRORD data. This suggests that their fit to the TG signal using a time-independent *D* may improve with the introduction of another intermediate.

Why is the activation process significantly faster for LOV2 than for other light-sensing proteins such as phytochrome (*29*) and PYP (*30*, *31*)? The relative simplicity of the LOV2 photocycle may be the key to understanding why the observed secondary structure unfolding is so comparatively fast ($\tau \sim 90$ μs for LOV2; $\tau = 2$ ms for PYP; and $\tau >$ 42 ms for phytochrome). In the early stages of the photocycles, there is an initial photoisomerization of the dark *trans-p*-hydroxycinnamic acid in PYP, for example, versus an initial singlet to triplet decay of the FMN group in LOV2. Aside from the LOV2 singlet excited state, there are no intermediates that precede formation of the FMN triplet (*11*). However, for PYP, several precursors to the pR_{465}[4] intermediate, which forms within a few nanoseconds (*32*), have been observed. After pR_{465} has formed, a transfer of an intramolecular proton from Glu46 (pB_{355}', $\tau = 250$ μs) occurs before the final formation of the signaling state, pB_{355} ($\tau =$ 2 ms). By comparison, there are no additional intermediates between the FMN triplet state and the partially unfolded 90 μs intermediate.

pB_{355}' plays a key role in facilitating the secondary structure changes during formation of the pB_{355} signaling state in PYP. According to Xie et al. (*31*), the buried charge group, COO^- from Glu46, found in the pB_{355}' intermediate drives large global protein structural changes. The importance of this buried charge group is underscored by the reduction in the extent of conformational changes observed in the E46QA mutant. Thus, the relatively long time required for the transition from pR_{465} to pB_{355} is explained in part by the time ($\tau = 250$ μs) required to form pB_{355}' (*31*) and in part by the high energy barrier that faces the chromophore as its phenolic oxygen passes from one side of the ring plane to the other (*33*). Such similar steric factors must be absent from the LOV2 photocycle mechanism. The FMN moiety is initially noncovalently bound, with its C(4a) 4.2 Å from the sulfur of Cys39 (*34*). Illumination brings about a rotation of the sulfur group by 100° around the $C_\alpha - C_\beta$ bond. This action readies the Cys39 sulfur for formation of a bond with C(4a) by moving it 2.3 Å so that it is within covalent bonding distance. Subsequent to adduct formation, in the presence of the Jα helix, NMR experiments have reported significant perturbations at that helix (*9*, *10*). Upon formation of the adduct, there are significant changes in the environment of amino acid residues in the Gβ, Hβ, and Iβ strands, as well as the Eα helix. Because the Jα helix, which lies beneath the chromophore, interacts with several strands of the β-sheet surface of the LOV domain, these localized changes in the β-strands are then proposed to relay the blue light information further to the Jα helix. The relative proximity of these key elements may facilitate fast structural communication that explains why the kinetics of FMN adduct formation and the putative Jα helix unfolding follow closely in time. The unfolded Jα helix and the β-sheet face that is exposed upon Jα helix unfolding have been proposed to be surfaces that can play a role in kinase activation (*10*).

In conclusion, these TRORD and TROD experiments reveal a previously unreported intermediate species ($\tau \sim 90$ μs, $LOV2_{390}^{S2}$) that is characterized by a FMN adduct chromophore and partly unfolded secondary structure. Figure 3 summarizes the different kinetic intermediates that are currently observed in the LOV2 photocycle. $LOV2_{390}^{S2}$ appears shortly after the formation of the FMN adduct ($LOV2_{390}^{S1}$). For LOV2, the species that is ready to interact with a receptor domain for downstream signaling forms much faster than in other light-sensing proteins. The slower transition between the chromophore changes and the protein unfolding (in PYP and phytochrome) are likely due to higher energy barriers faced by the chromophore before it can communicate with the protein. In addition, the differences may arise from the nature of the receptor protein. That is, LOV2 may be designed to respond quickly to blue light illumination because it interacts with a kinase domain that is also within the phot1 photoreceptor. It might be that the sequential chromophore and protein responses to blue light in the LOV2 photocycle are common in the photocycles of PAS, as well as non-PAS, signaling proteins.

[4] There are at least two nomenclatures used to describe the PYP intermediates: pR_{465} (I_1), pB_{355} (I_2), and pB_{355}' (I_2'). In this paper, we will use pR and pB.

ACKNOWLEDGMENT

We thank Robert A. Goldbeck, Istvan Szundi, and James W. Lewis for assistance with data analysis and interpretation and Winslow Briggs and John Christie for a critical review of the paper.

REFERENCES

1. Huala, E., Oeller, P. W., Liscum, E., Han, I.-S., Larsen, E., and Briggs, W. R. (1997) *Arabidopsis* NPH1: A protein kinase with a putative redox-sensing domain, *Science 278*, 2120−2123.
2. Jarillo, J. A., Gabrys, H., Capel, J., Alonso, J. M., Ecker, J. R., and Cashmore, A. R. (2001) Phototropin-related NPL1 controls chloroplast relocation induced by blue light, *Nature 410*, 952−954.
3. Kagawa, T., Sakai, T., Suetsugu, N., Oikawa, K., Ishiguro, S., Kato, T., Tabata, S., Okada, K., and Wada, M. (2001) *Arabidopsis* NPL1: A phototropin homolog controlling the chloroplast high-light avoidance response, *Science 291*, 2138−2141.
4. Sakai, T., Kagawa, T., Kasahara, M., Swartz, T. E., Christie, J. M., Briggs, W. R., Wada, M., and Okada, K. (2001) *Arabidopsis* nph1 and npl1: Blue light receptors that mediate both phototropism and chloroplast relocation, *Proc. Natl. Acad. Sci. U.S.A. 98*, 6969−6974.
5. Kinoshita, T., Doi, M., Suetsugu, N., Kagawa, T., Wada, M., and Shimazaki, K. (2001) Phot1 and phot2 mediate blue light regulation of stomatal opening, *Nature 414*, 656−660.
6. Christie, J. M., and Briggs, W. R. (2005) Blue light sensing and signaling by the phototropins, in *Handbook of Photosensory Receptors* (Briggs, W. R., and Spudich, J. L., Eds.) pp 277−303, Wiley-VCH, Weinheim, Germany.
7. Swartz, T. E., Corchnoy, S. B., Christie, J. M., Lewis, J. W., Szundi, I., Briggs, W. R., and Bogomolni, R. A. (2001) The photocycle of a flavin-binding domain of the blue light photoreceptor phototropin, *J. Biol. Chem. 276*, 36493−36500.
8. Corchnoy, S. B., Swartz, T. E., Lewis, J. W., Szundi, I., Briggs, W. R., and Bogomolni, R. A. (2003) Intramolecular proton transfers and structural changes during the photocycle of the LOV2 domain of phototropin 1, *J. Biol. Chem. 278*, 724−731.
9. Harper, S. M., Neil, L. C., and Gardner, K. H. (2003) Structural basis of a phototropin light switch, *Science 301*, 1541−1544.
10. Harper, S. M., Christie, J. M., and Gardner, K. H. (2004) Disruption of the LOV-Jα helix interaction activates phototropin kinase activity, *Biochemistry 43*, 16184−16192.
11. Kennis, J. T. M., Crosson, S., Gauden, M., van Stokkum, I. H. M., Moffat, K., and van Grondelle, R. (2003) Primary reactions of the LOV2 domain of phototropin, a plant blue-light photoreceptor, *Biochemistry 42*, 3385−3392.
12. Salomon, M., Christie, J. M., Knieb, E., Lempert, U., and Briggs, W. R. (2000) Photochemical and mutational analysis of the FMN-binding domains of the plant blue light receptor, phototropin, *Biochemistry 39*, 9401−9410.
13. Rajagopal, S., Anderson, S., Šrajer, V., Schmidt, M., Pahl, R., and Moffat, K. (2005) A structural pathway for signaling in the E46Q mutant of photoactive yellow protein, *Structure 13*, 55−63.
14. Cherry, J. R., Hondred, D., Walker, J. M., and Vierstra, R. D. (1992) Phytochrome requires the 6-kDa N-terminal domain for full biological activity, *Proc. Natl. Acad. Sci. U.S.A. 89*, 5039−5043.
15. Wang, H., and Deng, X. W. (2002) Phytochrome signaling mechanism, in *The Arabidopsis Book* [Online] (Somerville, C. R., and Meyerowitz, E. M., Eds.) American Society of Plant Biologists, Rockville, MD, http://www.aspb.org/publications/arabidopsis/ (accessed April 4, 2002).
16. Gong, W., Hao, B., Mansy, S. S., Gonzalez, G., Gilles-Gonzalez, M. A., and Chan, M. K. (1998) Structure of a biological oxygen sensor: A new mechanism for heme-driven signal transduction, *Proc. Natl. Acad. Sci. U.S.A. 95*, 15177−15182.
17. Key, J., and Moffat, K. (2005) Crystal structures of deoxy and CO-bound *bj*FixLH reveals details of ligand recognition and signaling, *Biochemistry 44*, 4627−4635.
18. Zhang, R.-G., Pappas, T., Brace, J. L., Miller, P. C., Oulmassov, T., Molyneaux, J. M., Anderson, J. C., Bashkin, J. K., Winans, S. C., and Joachimiak, A. (2002) Structure of a bacterial quorum-sensing transcription factor complexed with pheromone and DNA, *Nature 417*, 971−974.
19. Vannini, A., Volpari, C., Gargioli, C., Muraglia, E., Cortese, R., De Francesco, R., Neddermann, P., and Di Marco, S. (2002) The crystal structure of the quorum sensing protein TraR bound to its autoinducer and target DNA, *EMBO J. 21*, 4393−4401.
20. Morais Cabral, J. H., Lee, A., Cohen, S. L., Chait, B. T., Li, M., and Mackinnon, R. (1998) Crystal structure and functional analysis of the HERG potassium channel N terminus: A eukaryotic PAS domain, *Cell 95*, 649−655.
21. Christie, J. M., Salomon, M., Nozue, K., Wada, M., and Briggs, W. R. (1999) LOV (light, oxygen, or voltage) domains of the blue-light photoreceptor phototropin (nph1): Binding sites for the chromophore flavin mononucleotide, *Proc. Natl. Acad. Sci. U.S.A. 96*, 8779−8783.
22. Nakasako, M., Iwata, T., Matsuoka, D., and Tokutomi, S. (2004) Light-induced structural changes of LOV domain-containing polypeptides from *Arabidopsis* phototropin 1 and 2 studied by small-angle X-ray scattering, *Biochemistry 43*, 14881−14890.
23. Nakasone, Y., Eitoku, T., Matsuoka, D., Tokutomi, S., and Terazima, M. (2006) Kinetic measurement of transient dimerization and dissociation reactions of *Arabidopsis* phototropin 1 LOV2 domain, *Biophys. J. 91*, 645−653.
24. Shapiro, D. B., Goldbeck, R. A., Che, D., Esquerra, R. M., Paquette, S. J., and Kliger, D. S. (1995) Nanosecond optical rotatory dispersion spectroscopy: Application to photolyzed hemoglobin-CO kinetics, *Biophys. J. 68*, 326−334.
25. Goldbeck, R. A., and Kliger, D. S. (1993) Nanosecond time-resolved absorption and polarization, *Methods Enzymol. 226*, 147−177.
26. Guo, H., Kottke, T., Hegemann, P., and Dick, B. (2005) The phot LOV2 domain and its interaction with LOV1, *Biophys. J. 89*, 402−412.
27. Eitoku, T., Nakasone, Y., Matsuoka, D., Tokutomi, S., and Terazima, M. (2005) Conformational dynamics of phototropin 2 LOV2 domain with the linker upon photoexcitation, *J. Am. Chem. Soc. 127*, 13238−13244.
28. Choi, J., and Terazima, M. (2003) Energy and volume changes induced by photoinitiated proton releasing reaction with apomyoglobin, *Rev. Sci. Instrum. 74*, 319−321.
29. Chen, E., Parker, W., Lewis, J. W., Song, P.-S., and Kliger, D. S. (1993) Time-resolved UV circular dichroism of phytochrome A: Folding of the N-terminal region, *J. Am. Chem. Soc. 115*, 9854−9855.
30. Chen, E., Gensch, T., Gross, A. B., Hendriks, J., Hellingwerf, K. J., and Kliger, D. S. (2003) Dynamics of protein and chromophore structural changes in the photocycle of photoactive yellow protein monitored by time-resolved optical rotatory dispersion, *Biochemistry 42*, 2062−2071.
31. Xie, A., Kelemen, L., Hendriks, J., White, B. J., Hellingwerf, K. J., and Hoff, W. D. (2001) Formation of a new buried charge drives a large-amplitude protein quake in photoreceptor activation, *Biochemistry 40*, 1510−1517.
32. Ujj, L., Devanathan, S., Meyer, T. E., Cusanovich, M. A., Tollin, G., and Atkinson, G. H. (1998) New photocycle intermediates in the photoactive yellow protein from *Ectothiorhodospira halophila*: Picosecond transient absorption spectroscopy, *Biophys. J. 75*, 406−412.
33. Perman, B., Šrajer, V., Ren, Z., Teng, T.-Y., Pradervand, C., Ursby, T., Bourgeois, D., Schotte, F., Wulff, M., Kort, R., Hellingwerf, K., and Moffat, K. (1998) Energy transduction on the nanosecond time scale: Early structural events in a xanthopsin photocycle, *Science 279*, 1946−1950.
34. Crosson, S., and Moffat, K. (2002) Photoexcited structure of a plant photoreceptor domain reveals a light-driven molecular switch, *Plant Cell 14*, 1067−1075.

BI602544N